Supplemental Figure 1. Clinical characteristics of ClinSeq™ participants by rs1260326 genotype. Unadjusted trait values for ClinSeq™ participants separated by *GCKR* genotype for (A) triglycerides and (B) fasting glucose. Red bars = unadjusted means ± SD. Two-tailed p-values are compared to WT (see also Supplemental Table 1). *WT, individuals homozygous for Pro at position 446; P446L, heterozygous individuals at position 446; L446, individuals homozygous for Leu at position 446.*

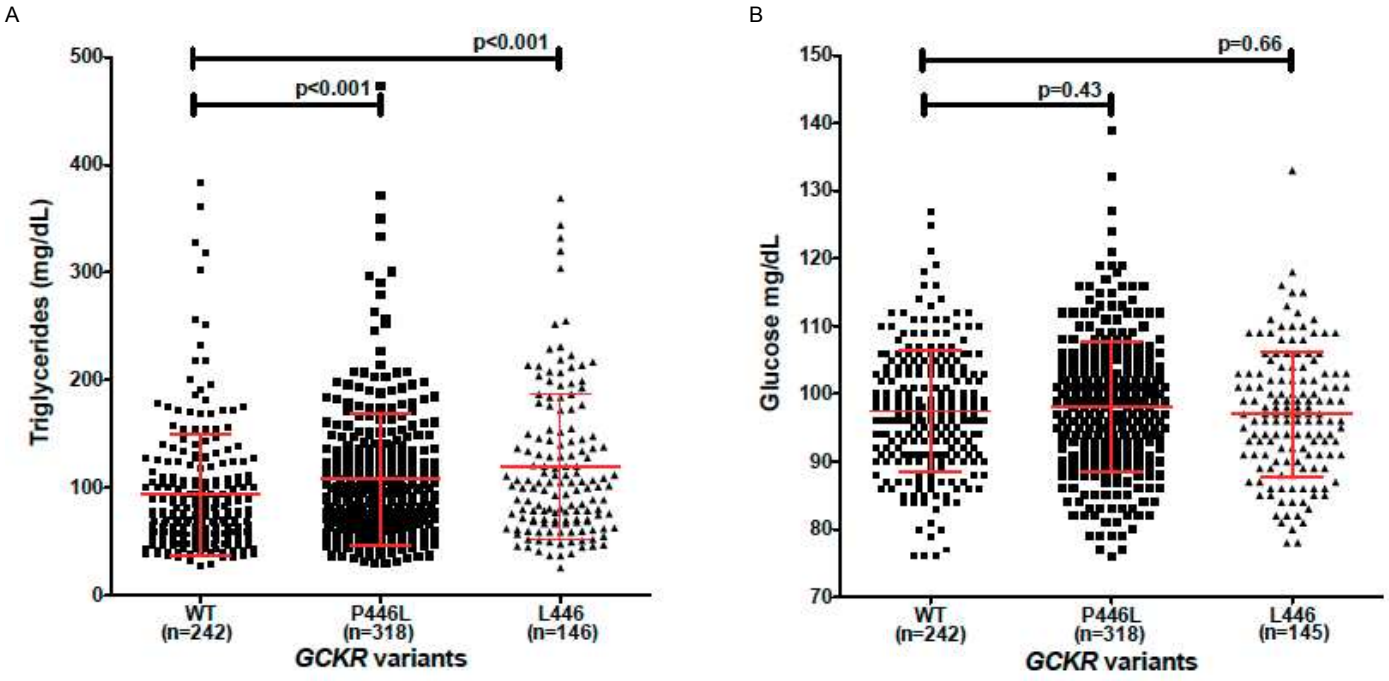

Supplemental Figure 2. Protein domains and bacterial homology of GKRP.
(A) The location of ClinSeq™ variants are shown relative to the two sugar isomerase domains (SIS 1 and SIS 2). The boundaries of SIS domains were predicted using a Conserved Domains search (http://www.ncbi.nlm.nih.gov/Structure/cdd/wrpsb.cgi). Putative sugar binding motifs (1) within SIS domains are shown as bold lines. Nonsense and frameshift variants are shown in red.

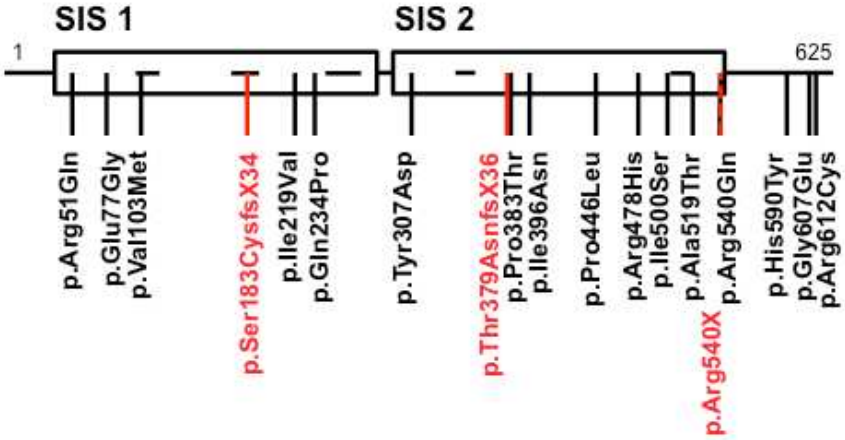

(B) Manual alignment of human GKRP residues 209-278 with *H. influenzae* YfeU residues 162-208 and human GKRP residues 481-519 with YfeU residues 206-244. The predicted secondary structure (2) for human GKRP is shown above the alignment. Secondary structure from the X-ray structure of YfeU is shown below the alignment (3). Conserved residues are in red. Residues that did not align by sequence or structure homology are in lowercase. Predicted sugar binding motifs (1) are identified in green. Ile219, Gln234, and Ile500 are highlighted in yellow. *helix = alpha-helical region; strand = beta-strand region; loop = neither helix nor sheet.*

```
hGKRP  loop-- -->helix--------------- ->   str-loop------------>helix--------->
  209  NPVSMA rndpiedwsstfrqvaermqkmq EKQKAFVLNPAI GPEGLSGSSRMKGGSATKILLETLLLAAH
  162  NPKSAA                         SEIADIAIETIV GPEILTGSSRLKAGTAQKMVLNMLSTASM
 YfeU  loop--                         ---->str-loop--------->helix--------------
                                                 motif C---------------->

 hGKRP
   481  STKWVLNTVSTGAHVLLGKILQNHMLDLRISNSKLFWRA
   206  AQKMVLNMLTTASMILLGKCYENLMVDVQASNEKLKARA
  YfeU                       motif E---------->
```

(C) Helical wheel diagram of human GKRP residues 218-236. Ile219 and Gln234 are boxed in black.
yellow circles = hydrophobic residues; blue circles = polar uncharged residues; green = positively charged residues; purple = negatively charged residues; red = residue unfavorable for helix formation

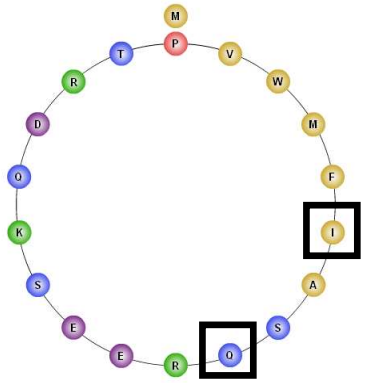

Image generated from:
http://www-nmr.cabm.rutgers.edu/bioinformatics/Proteomic_tools/Helical_wheel/

Supplemental Figure 3. Fluorescence imaging of YFP-GKRP variants with and without co-expression of CFP-GCK.
All images are representative of transfections performed at least twice from two independent plasmid preparations per variant. Images were taken at 63x magnification using the same laser settings and intensity.

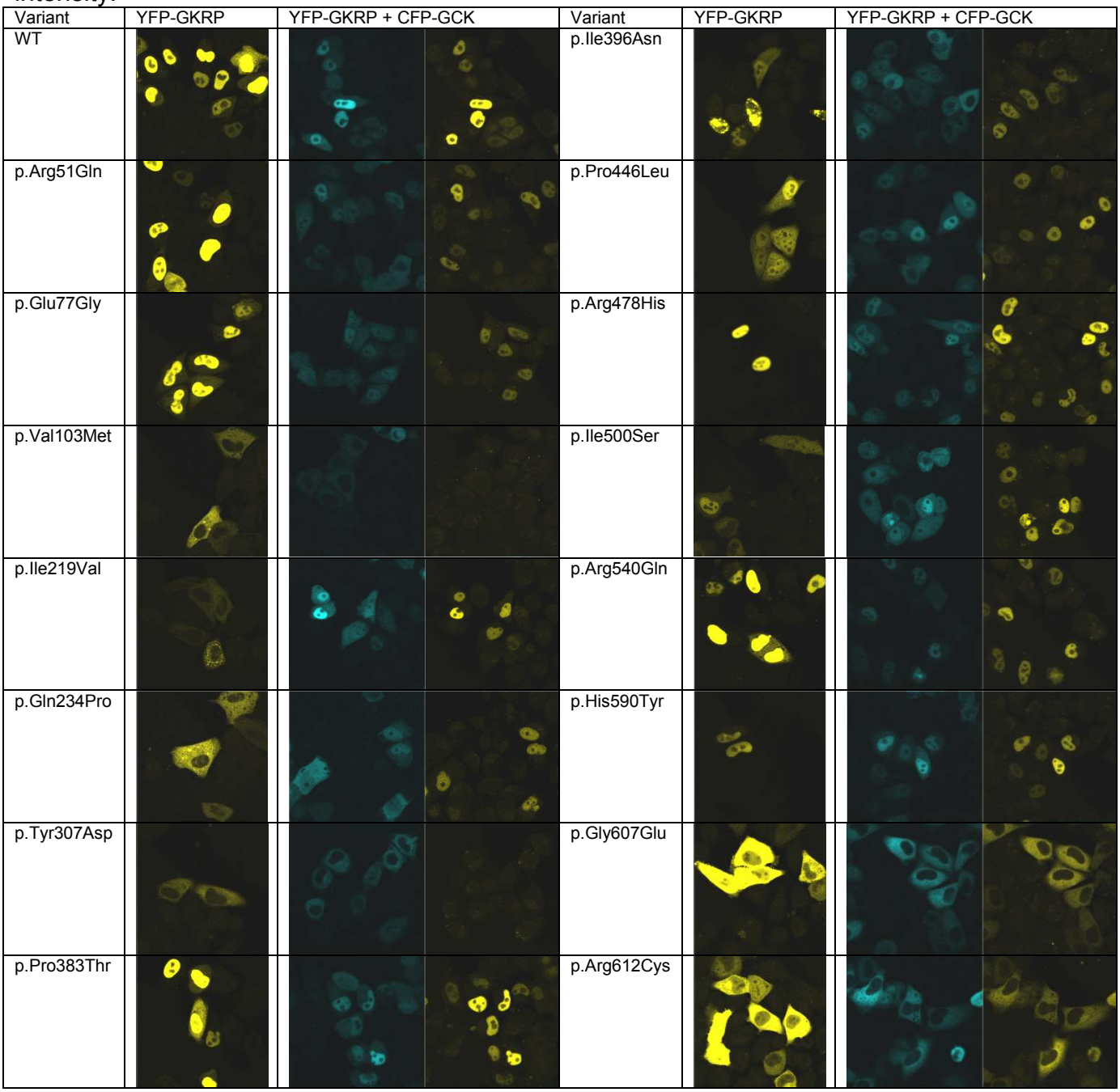

Supplemental Figure 4. Effect of Leu446 in *cis* on rare variants p.Glu77Gly, p.Pro383Thr, and p.Arg540Gln.

p.[Glu77Gly; Pro446Leu] and p.[Pro383Thr; Pro446Leu] showed near-complete cytoplasmic expression while p.[Pro446Leu; Arg540Gln] showed mixed nuclear and cytoplasmic localization similar to p.Pro446Leu alone. All images were taken at 63x magnification using the same laser settings and intensity and are representative of at least two transfections of two independent plasmid preparations for each variant.

p.[Glu77Gly; Pro446Leu] p.[Pro383Thr; Pro446Leu] p.[Pro446Leu; Arg540Gln]

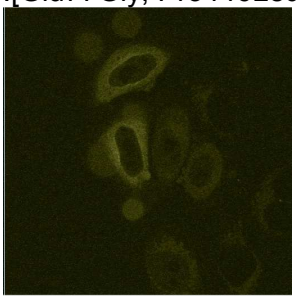
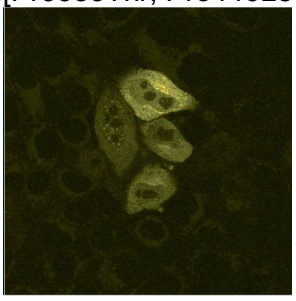
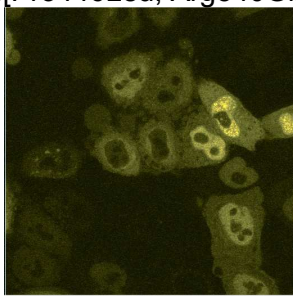

Supplemental Figure 5. Transient transfection of a plasmid containing YFP-tagged *Xenopus laevis* GKRP and CFP-tagged human liver GCK in HeLa cells.

Xenopus GKRP (*right*) localized primarily to the nucleus after 72 hours and was competent to sequester human GCK (*left*) to some degree. The image was taken at 63x magnification using the same laser settings and intensity as in Supplemental Figure 3.

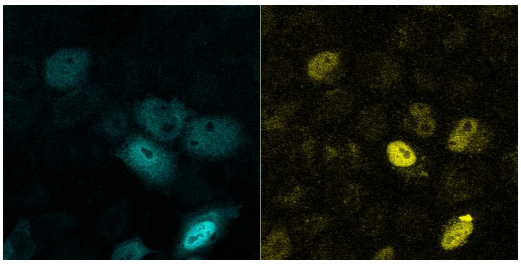

Supplemental Figure 6. Effect of glucose on 10 mU/ml GCK in the absence and presence of one unit of WT and variant GKRP proteins.
No significant difference was observed between (A) WT GKRP and p.Arg612Cys-GKRP ($p > 0.05$ and $n = 12$), (B) WT GKRP and p.Pro383Thr-GKRP ($p > 0.05$ and $n = 6$), (C) WT GKRP and p.Ile219Val-GKRP ($p > 0.05$ and $n = 6$), (D) WT GKRP and p.Ile500Ser-GKRP ($p > 0.05$ and $n = 6$) and (E) WT GKRP and p.Gln234Pro-GKRP ($p > 0.05$ and $n = 42$). GCK activity is plotted as a percentage of that obtained in the absence of regulatory protein at 100 mM glucose. Data points are mean ± SEM.

A

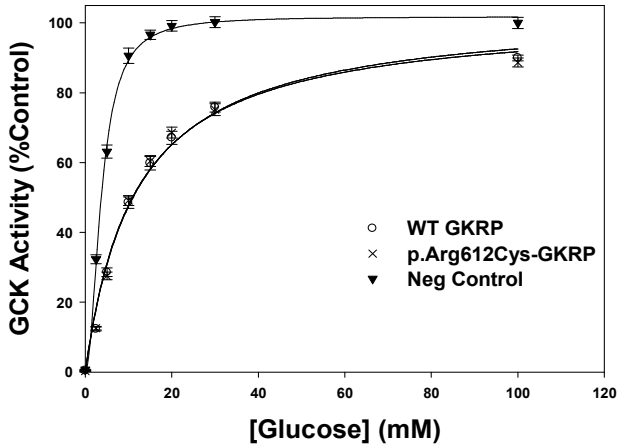

B

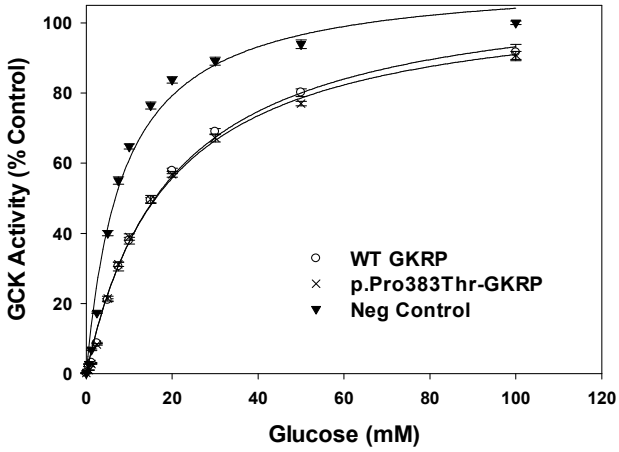

C

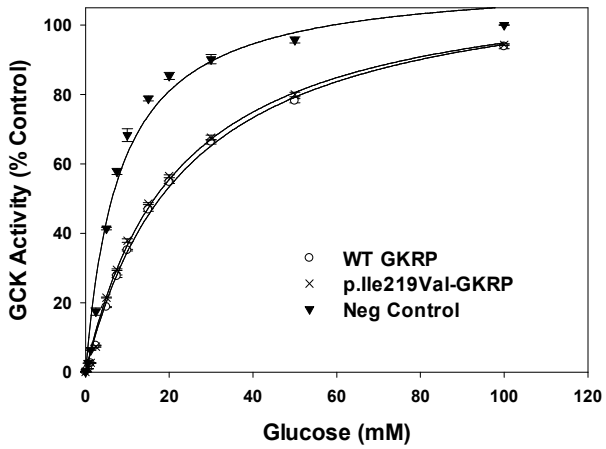

D

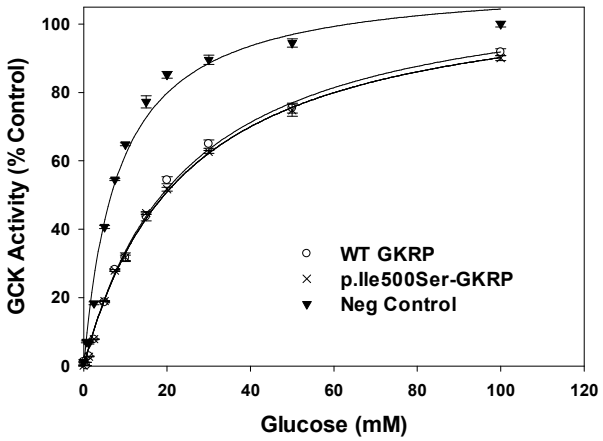

E

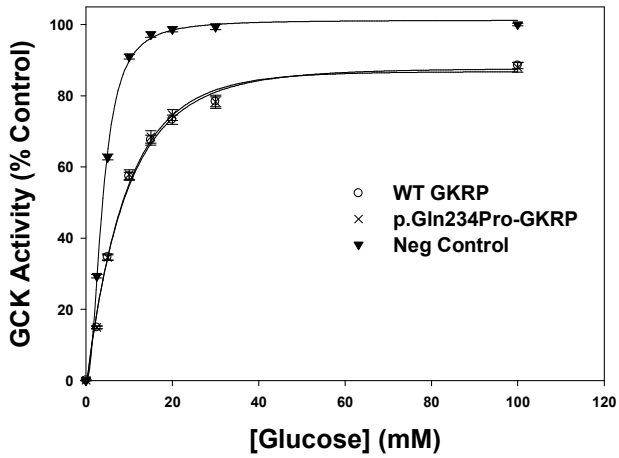

Supplemental Figure 7. Assessment of the p.Pro383Thr variant in conjunction with p.Pro446Leu. (A) Activity comparisons of p.Pro383Thr-GKRP and p.[Pro383Thr; Pro446Leu]-GKRP. (B) Response of p.[Pro383Thr; Pro446Leu]-GKRP to F1P and F6P in comparison to p.Pro446Leu-GKRP. GCK activity is plotted as a percentage of that obtained in the absence of regulatory protein at 5 mM glucose. Data points are mean ± SEM. * $p < 0.05$; ** $p < 0.01$; *** $p < 0.001$

A

Protein	Protein activity (µg/ml)
Wild-type	2.85
p.Pro446Leu	3.24
p.Pro383Thr	3.00
p.[Pro383Thr; Pro446Leu]	4.13

B

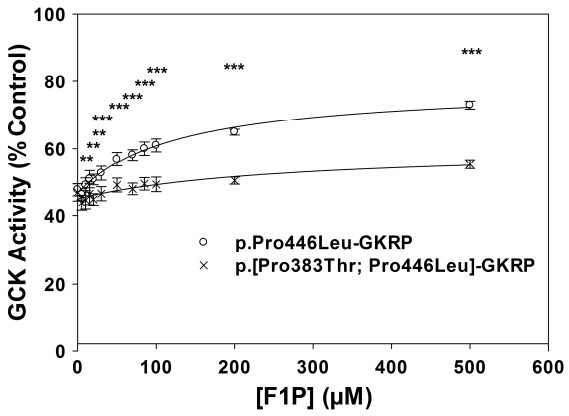

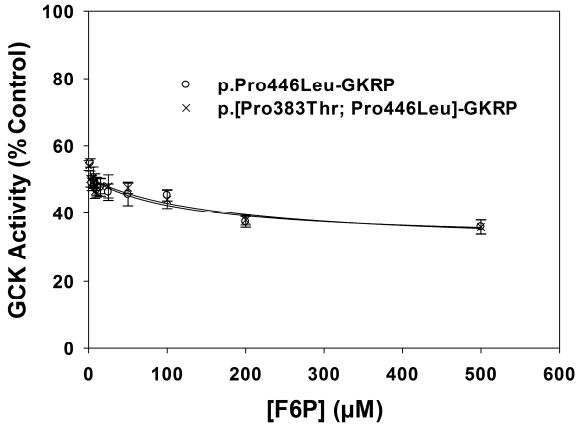

Supplemental Figure 8. Lipid levels of ClinSeq™ participants by *GCKR* genotype. Unadjusted trait values for ClinSeq™ participants separated by *GCKR* genotype for (A) triglycerides, (B) total cholesterol and (C) LDL cholesterol. Red bars = unadjusted means ± SD. Two-tailed p-values are compared to WT (see also Table 3). *WT, individuals homozygous for Pro at position 446; P446L, heterozygous individuals at position 446; L446, individuals homozygous for Leu at position 446; rare, individuals heterozygous for one or more rare* GCKR *nonsynonymous variants; WT-like, individuals heterozygous for rare* GCKR *nonsynonymous variants with cellular localization indistinguishable from wild-type; LOF, individuals heterozygous for rare* GCKR *nonsynonymous variants with predicted or observed cellular localization defect, reduced protein expression, and/or a kinetic defect.*

A

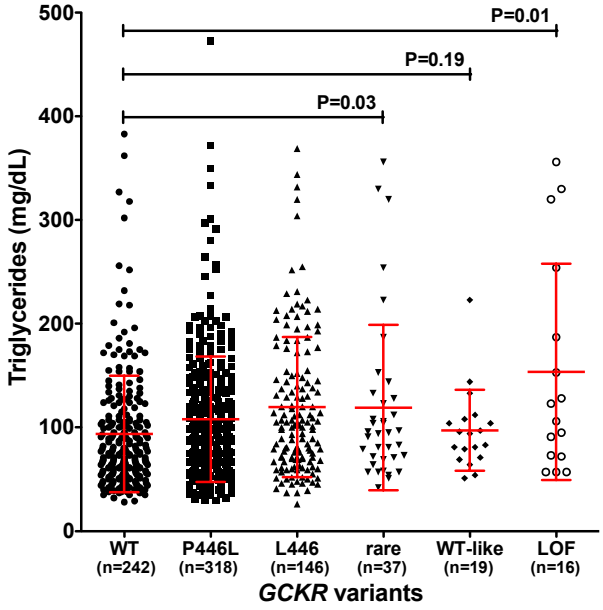

B

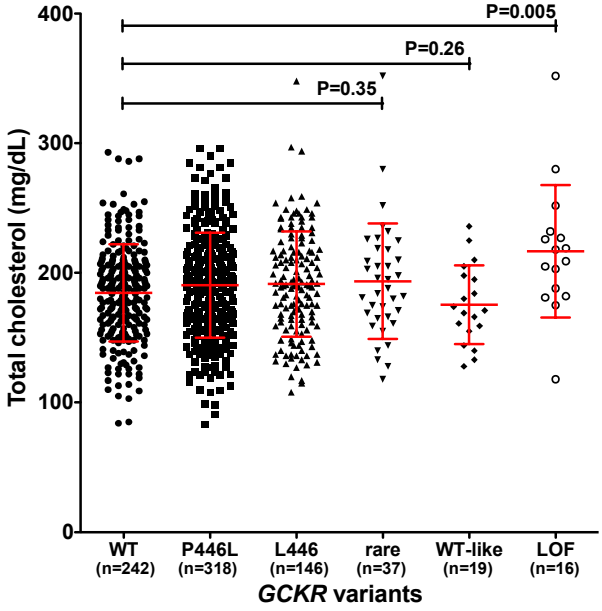

C

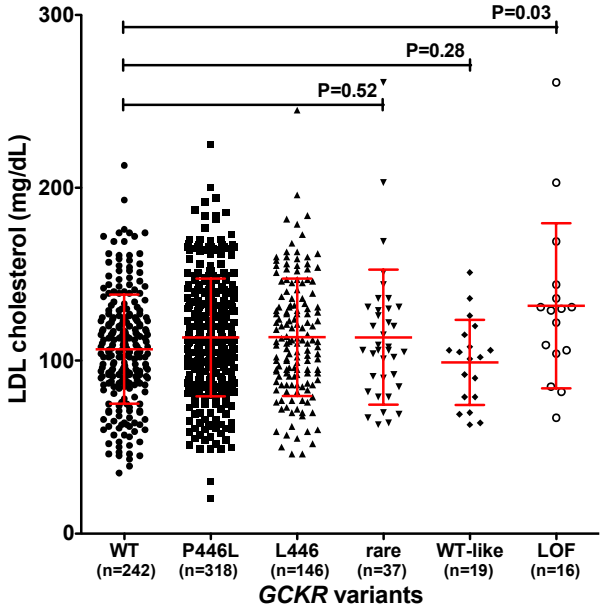

Supplemental Figure 9. Further separation of rare *GCKR* variants by biochemical effect. Unadjusted trait values for ClinSeq™ participants separated by *GCKR* genotype for triglycerides, total cholesterol, BMI and fasting insulin. Red bars = unadjusted means. *GOF, individuals heterozygous for a putative C-terminal gain-of-function rare* GCKR *nonsynonymous variant; WT-like, individuals heterozygous for rare* GCKR *nonsynonymous variants with cellular localization indistinguishable from wild-type; mild LOF, individuals heterozygous for rare* GCKR *nonsynonymous variants with a cellular localization defect, reduced protein expression, and/or a kinetic defect; severe LOF, individuals heterozygous for rare* GCKR *nonsynonymous variants with most severe effects on protein expression and/or kinetic parameters (p.Val103Met, p.[Ser183CysfsX34; Ala519Thr], p.[Gln234Pro; Arg540X], p.Tyr307Asp, p.Thr379AsnfsX36, p.Pro383Thr, p.Ile500Ser)*

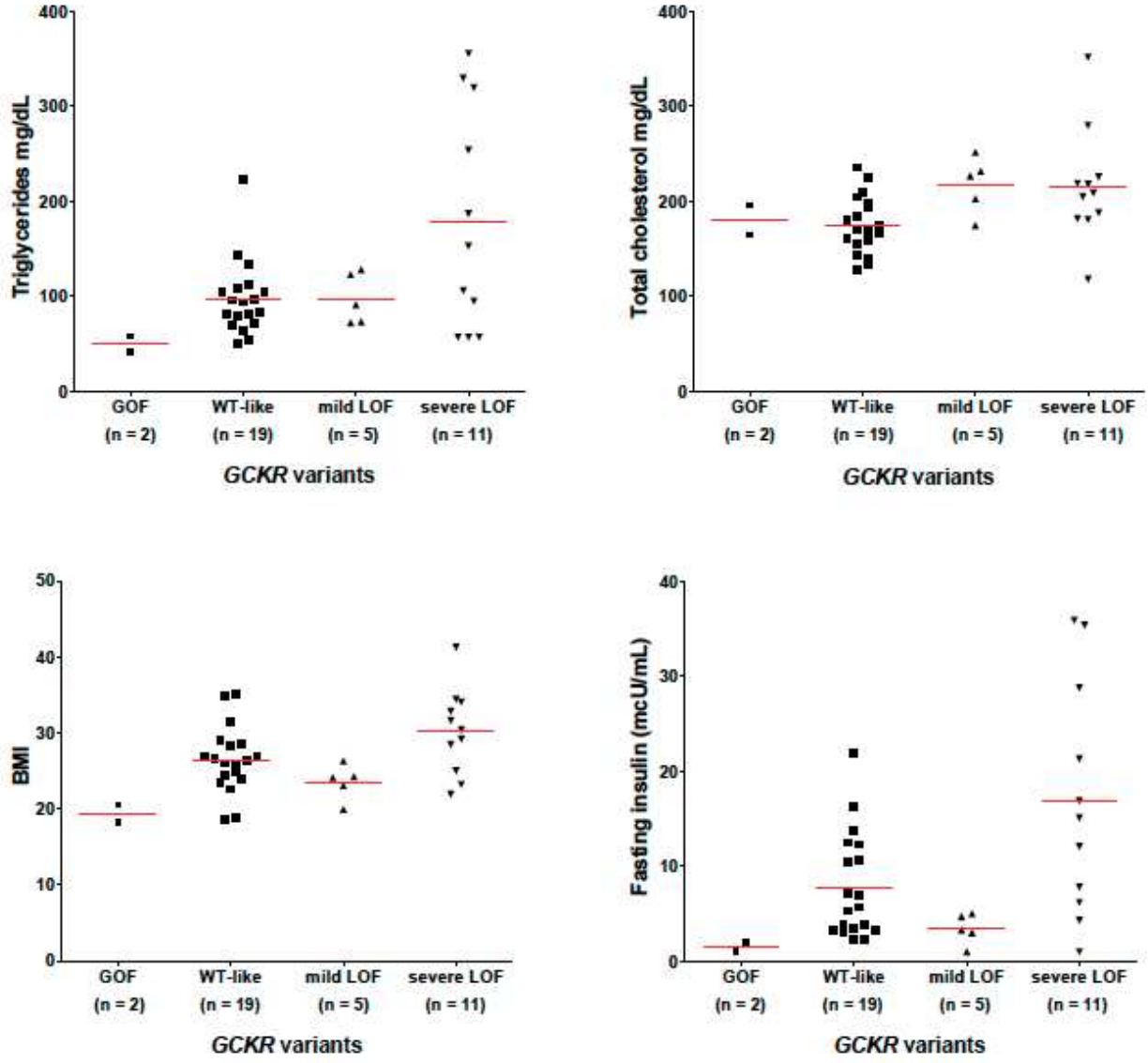

Supplemental Table 1. Selected mean baseline clinical characteristics of ClinSeq™ individuals separated by rs1260326 genotype

Clinical features	***GCKR* WT mean±SD** n = 242	***GCKR* P446L mean±SD** n = 318	***GCKR* L446 mean±SD** n = 146	**P446L vs WT *P* (2-tailed)**	**L446 vs WT *P* (2-tailed)**
Age (years)	56.6±5.5	56.0±5.6	56.2±5.6	0.23	0.49
Sex (% female)	55.8%	52.8%	55.5%	0.49	1.00
T2D exclusion (%)	8.3%	5.4%	4.6%	0.19	0.17
BMI (kg/m^2)	27.0±4.5	27.0±4.9	27.3±5.3	0.79	0.75
Fasting glucose (mg/dL)	97.4±9.0	98.1±9.7	97.0±9.2	0.43	0.66
Fasting insulin (mcU/mL)	8.9±6.3	9.3±7.1	8.8±6.6	1.00	0.67
C-peptide (ng/mL)	2.2±1.1	2.3±1.2	2.2±1.2	0.73	0.79
CRP (mg/dL)	0.21±0.31	0.26±0.46	0.25±0.27	0.15	0.05
Total cholesterol (mg/dL)	184.6±37.5	190.5±40.5	191.4±40.6	0.09	0.15
HDL cholesterol (mg/dL)	60.0±16.3	58.0±16.5	56.7±15.8	0.13	0.07
LDL cholesterol (mg/dL)	106.7±31.6	113.4±34.0	113.6±34.0	0.04	0.08
Triglycerides (mg/dL)	93.8±56.2	108.0±60.5	119.6±67.6	<0.001	<0.001

GCKR subgroups were defined as: *GCKR* WT (individuals who are homozygous for Pro at position 446), *GCKR* P446L (individuals who are heterozygous for p.Pro446Leu), and *GCKR* L446 (individuals who are homozygous for Leu at position 446). Fisher's exact test was used to compare differences in frequency distribution of sex and prevalence of type 2 diabetes among the *GCKR* subgroups. The Mann-Whitney U test was used for pair-wise comparison of unadjusted means in all other clinical variables among the *GCKR* subgroups. Individuals with potential familial hyperlipidemia and those with type 2 diabetes were excluded from phenotype analysis.

Supplemental Table 2. p.Pro446Leu genotype and phase of Leu446 for individuals with rare *GCKR* variants.

Amino acid change	Number of individuals	p.Pro446Leu genotype	Leu446 phase
p.Arg51Gln	4	3 Pro/Pro	Trans
		1 Pro/Leu	
p.Glu77Gly	1	Leu/Leu	Cis
p.Val103Met	2	2 Pro/Leu	Trans
p.[Ser183CysfsX34; Ala519Thr]	3	2 Pro/Pro	Trans
		1 Pro/Leu	
p.[Ser183CysfsX34; Ala519Thr];[Arg540Gln]	1	Pro/Leu	Trans
p.Ile219Val	1	Pro/Leu	***Unknown***
p.Gln234Pro	3	Pro/Pro	
p.[Gln234Pro; Arg540X]	1	Pro/Leu	Trans
p.[Tyr307Asp(;)Arg540Gln]	1	Pro/Leu	***Unknown***
p.Thr379AsnfsX36	2	2 Pro/Leu	Trans
p.Pro383Thr	1	Pro/Leu	Cis
p.Ile396Asn	1	Pro/Leu	Trans
p.Arg478His	1	Pro/Pro	
p.Ile500Ser	1	Pro/Leu	***Unknown***
p.Arg540Gln	15	12 Pro/Leu	Cis
		3 Leu/Leu	
p.His590Tyr	2	2 Pro/Leu	***Unknown***
p.Gly607Glu	1	Pro/Pro	
p.Arg612Cys	1	Pro/Leu	Trans

Supplemental Table 3. Mammalian conservation of *GCKR* variants from the ClinSeq™ project.

	p.Arg51Gln	p.Glu77Gly	p.Val103Met	p.Ile219Val	p.Gln234Pro	p.Tyr307Asp	p.Pro383Thr	p.Ile396Asn	p.Pro446Leu	p.Arg478His	p.Ile500Ser	p.Arg540Gln	p.His590Tyr	p.Gly607Glu	p.Arg612Cys
P. troglodytes	R	E	V	I	Q	Y	P	I	P	R	I	R	H	G	R
P. abelii	R	E	V	I	Q	Y	P	I	P	R	I	R	H	G	R
M. mulatta	R	E	V	I	Q	Y	P	I	P	R	I	R	H	G	R
A. melanoleuca	R	E	V	I	Q	Y	P	I	P	H	I	Q	Q	G	R
C. famliaris	R	E	V	I	Q	Y	P	I	P	H	I	Q	H	G	R
E. caballus	Q	D	V	I	Q	Y	P	I	P	H	I	Q	H	G	R
O. cuniculus	Q	E	V	I	Q	Y	P	I	P	R	I	Q	H	G	R
M. musculus	Q	E	V	I	Q	Y	P	V	P	R	I	Q	R	G	R
R. norvegicus	K	E	V	I	Q	Y	P	I	P	R	I	Q	R	G	R

Sequences are from protein BLAST (http://blast.ncbi.nlm.nih.gov/Blast.cgi) of human GKRP (accession no. Q14397). All mammalian species with full-length alignments to human GKRP are shown. In cases where more than one sequence aligned per species, only the sequence with highest homology was selected. Mammalian species were chosen because non-mammalian homologues (as is the case for *Xenopus laevis* GKRP) may not respond to phosphate esters F1P and F6P.

Supplemental Table 4. Comparison of biochemical defects with SIFT and PolyPhen predictions of human missense variant severity.

Variant	SIFT prediction	PolyPhen prediction	Functional assessment	Agreement
p.Arg51Gln	Tolerated	benign	Benign	BOTH
p.Glu77Gly	Tolerated	benign	Benign	BOTH
p.Val103Met	affect protein function	probably damaging	Damaging	BOTH
p.Ile219Val	Tolerated	benign	Damaging	NEITHER
p.Gln234Pro	Tolerated	possibly damaging	Damaging	PolyPhen
p.Tyr307Asp	affect protein function	probably damaging	Damaging	BOTH
p.Pro383Thr	affect protein function	probably damaging	Damaging	BOTH
p.Ile396Asn	affect protein function	possibly damaging	Damaging	BOTH
p.Pro446Leu	affect protein function	benign	Damaging	SIFT
p.Arg478His	Tolerated	benign	Benign	BOTH
p.Ile500Ser	affect protein function	possibly damaging	Damaging	BOTH
p.Arg540Gln	Tolerated	benign	Benign	BOTH
p.His590Tyr	affect protein function	probably damaging	Benign	NEITHER
p.Gly607Glu	Tolerated	possibly damaging	Damaging	PolyPhen
p.Arg612Cys	affect protein function	probably damaging	Damaging	BOTH

Variants were assessed using the SIFT and PolyPhen algorithms (4, 5). Functional assessment was assigned as 'benign' for variants showing WT-like predominant nuclear localization as YFP-fusion proteins in HeLa cells and 'damaging' for variants with cellular and/or kinetic defects.

Supplemental Table 5. Conservation of C-terminal residues from GKRP orthologues experimentally validated to localize to the nucleus.

	Overall sequence identity	C-terminal sequence identity	595 605 615 625
H. sapiens			P**S**VCEAVR**S**ALAG**PG**Q**KR**TADPLEILEPDVQ----
R. norvegicus	89%	62%	S**S**VCEVVR**S**ALSG**PG**Q**KR**STQALE—DPPACGTLN
M. musculus	88%	59%	S**S**VCEVVR**S**ALSG**PG**Q**KR**SIQAFG--DPVVP----
X. laevis	59%	31%	L**S**IRSAIE**S**SMNV**PG**R**KR**GAEDSESR---------

Percentage identities and alignments were calculated using the ClustalW algorithm in MegAlign (Lasergene, DNASTAR). Sequences were from protein BLAST searches with human GKRP (http://blast.ncbi.nlm.nih.gov/). Residues conserved in all four species are **bold and underlined**.

Supplemental Table 6. Relative activity and maximal response to F1P or F6P of recombinant FLAG-tagged variant GKRP preparations compared to WT GKRP.

Protein	Relative activity	F6P amplitude ratio (WT GKRP / variant GKRP)	F1P amplitude ratio (WT GKRP / variant GKRP)
Wild-type	1	1	1
p.Ile219Val	0.88	N/S[A]	1.11
p.Gln234Pro	0.79	1.24	1.13
p.Pro383Thr	0.97	N/S	3.4
p.[Pro383Thr; Pro446Leu]	0.69	N/S	3.3
p.Pro446Leu	0.88	1.08	N/S
p.Ile500Ser	1.03	1.25	2.25
p.Arg612Cys	1.02	N/S	N/S

[A] no significant difference compared to WT GKRP

Supplemental Table 7. Modeling kinetic effects of either Pro446 or Leu446 in *trans.*

Protein	Relative concentration required for one unit activity	Relative concentration required for one unit activity, 500μM F6P	Relative amplitude of response to F1P
Wild-type	1	1	1
p.Pro383Thr	1.14	1.20	0.39
p.Pro446Leu	1.25	1.22	0.93
p.[Pro383Thr; Pro446Leu]	1.34	1.42	0.38
WT + p.Pro383Thr	1.06	1.14	0.71
WT + p.[Pro383Thr; Pro446Leu]	1.22	1.30	0.71
p.Pro446Leu + p.Pro383Thr	1.20	1.26	0.71
p.Pro446Leu + p.[Pro383Thr; Pro446Leu]	1.30	1.44	0.69

Supplemental Table 8. Adjusted (least-square) means separated by *GCKR* genotype.

Baseline measurements	*GCKR* WT mean±SEM n=232	*GCKR* P446L mean±SEM n=312	*GCKR* L446 mean±SEM n=141	P446L vs WT ***P***	L446 vs WT ***P***
CRP (mg/dL)	0.20±0.02		0.24±0.02		0.27
Total cholesterol (mg/dL)	182.5±2.3	190.4±2.0	191.3±2.8	0.009	0.02
HDL cholesterol (mg/dL)	58.8±0.9	57.7±0.8	56.5±1.2	0.39	0.11
LDL cholesterol (mg/dL)	105.6±2.0	113.5±1.7	113.9±2.4	0.003	0.01
Triglycerides (mg/dL)	94.4±3.5	106.8±3.0	118.4±4.9	0.008	<0.001

Baseline measurements	*GCKR* non-rare mean±SEM n=684	*GCKR* rare mean±SEM n=37	*GCKR* LOF mean±SEM n=16	*GCKR* rare Vs non-rare ***P***	*GCKR* LOF vs non-rare ***P***
Total cholesterol (mg/dL)	187.5±1.3	198.8±5.7	215.2±8.7	0.06	0.002
HDL cholesterol (mg/dL)	57.8±0.5	58.0±2.2	58.8±3.4	0.91	0.76
LDL cholesterol (mg/dL)	110.6±1.2	117.9±5.0	128.7±7.6	0.15	0.02
Triglycerides (mg/dL)	104.8±2.2	120.0±9.4	153.9±14.4	0.12	0.001

For common variant p.Pro446Leu, *GCKR* subgroups were defined as: *GCKR* WT (individuals who are homozygous for Pro at position 446), *GCKR* P446L (individuals who are heterozygous for p.Pro446Leu), and *GCKR* L446 (individuals who are homozygous for Leu at position 446). For rare *GCKR* variants, *GCKR* subgroups were defined as: *GCKR* non-rare (individuals without rare *GCKR* nonsynonymous variants), *GCKR* rare (individuals with one or more rare *GCKR* nonsynonymous variants, and *GCKR* LOF (individuals with putative rare *GCKR* loss-of-function nonsynonymous variants.

Supplemental Table 9. P-trend regression effect estimates separated by *GCKR* genotype.

Dependent variable	Leu446 allele est±SEM n=453	Rare est±SEM n=37	Rare, WT-like est±SEM n=19	Rare, LOF est±SEM n=16	Leu446 Allele ***P***	Rare ***P***	Rare, WT-like ***P***	Rare, LOF ***P***
Fasting glucose (mg/dL)	-0.19±0.5	-0.78±1.5	0.81±2.0	-2.05±2.2	0.68	0.60	0.69	0.36
Fasting insulin (mcU/mL)	-0.21±0.3	0.22±0.9	-1.94±1.2	2.85±1.4	0.48	0.82	0.12	0.04
C-peptide (ng/mL)	-0.02±0.1	-0.24±0.2	-0.30±0.2	-0.19±0.2	0.66	0.13	0.18	0.41
CRP (mg/dL)	0.02±0.02	-0.02±0.06	0.06±0.08	-0.11±0.1	0.32	0.73	0.48	0.23
Total cholesterol (mg/dL)	4.21±1.8	11.54±5.9	1.76±8.0	27.29±8.8	0.02	0.05	0.83	0.002
HDL cholesterol (mg/dL)	-1.06±0.7	0.41±2.3	0.94±3.1	1.15±3.4	0.13	0.86	0.76	0.74
LDL cholesterol (mg/dL)	4.05±1.6	7.05±5.1	-0.01±7.0	17.49±7.7	0.01	0.17	1.00	0.02
Triglycerides (mg/dL)	11.3±3.0	15.0±9.8	-11.4±13.1	50.09±14.7	<0.001	0.13	0.38	<0.001

The ClinSeq™ cohort was analyzed using P-trend linear regression to estimate the effect of the *GCKR* Leu446 allele or rare *GCKR* nonsynonymous variants. Rare *GCKR* variants were further subdivided into WT-like and LOF subgroups (see Table 2).

Supplemental Table 10. Results from genotyping of selected rare *GCKR* variants from the ClinSeq™ cohort.

Amino acid change	Nucleotide change	n (heterozygotes)	n (genotyped)	Ethnicity
p.Val103Met	c.307G>A	0	8524	Finns
		28	1528	Mexican-American
p.[Ser183CysfsX34; Ala519Thr]	c.[548_549del; 1555G>A]	0	12168	Finns/Germans
		15	1206	Ashkenazi
p.Gln234Pro	c.701A>C	2	9728	Finns
		4	1868	Germans
p.Thr379AsnfsX36	c.1135dup	7	10299	Finns
		7	1864	Germans

Supplemental Table 11. Genotyping results of severe loss-of-function variants separated by glycemic status.

Amino acid change	Nucleotide change	n (T2D)	Frequency (T2D)	n (IGT/IFG)	Frequency (IGT/IFG)	n (controls)	Frequency (controls)	*p* (chi-square)[A]
p.Val103Met	c.307G>A	16	0.0203	8	0.0237	4	0.0093	0.17
p.[Ser183CysfsX34; Ala519Thr]	c.[548_549del; 1555G>A]	13	0.007	N/A	-	2	0.0036	0.60
p.Thr379AsnfsX36	c.1135dup	7	0.0027	4	0.0022	5	0.0008	0.036

[A] two-tailed chi-square tests were used to compare the frequency of variants in controls to frequency of variants in individuals with impaired glycemia [type 2 diabetes, impaired glucose tolerance (IGT), or impaired fasting glucose (IFG)]

Supplemental methods

GCKR sequencing primers

Primer name	Forward primer	Primer name	Reverse primer	Exon	Amplicon size
GCKR-F1	CTCTTCAGGGGCCAAAGC	GCKR-R1	ATTGCCCTAGCAGTCGAACA	1	700
GCKR-F2	TCTTTCCCTAATATGCCCAGAG	GCKR-R2	GAACTTTCCCAGCCACCTGTA	2	544
GCKR-F3	AAGCCCTGTCCACATACCAG	GCKR-R3	ACCAGTTTGACTCCCATGTCTT	3	700
GCKR-F4, 5	CATTGCATGTATTTGTTCAATTTT	GCKR-R4, 5	AACTTGGCTTACCTGTCACCAC	4	698
GCKR-F5, 6	TGCGAGATTCCATGTAGGACT	GCKR-R5, 6	GAATGCTGGGGCTTTTATGTC	5, 6	700
GCKR-F6, 7	GAGTGTCTATCATGCACCAACAA	GCKR-R6, 7	TAGAATCCCTTCCCCATCTTC	6, 7	642
GCKR-F8	GCATTCTGAAGGGTTCTGATGC	GCKR-R8	CTCTTGCCTCTTCAATCCCTG	8	462
GCKR-F9	GCCTCTAAAAGTTCCAAAGCATA	GCKR-R9	CTAAGAAGGGCCACCCAATTTT	9	687
GCKR-F10	GGCCCTTCCCCTCTTTCTAA	GCKR-R10	CAGGCTCAGGGATTAGGTCTG	10	532
GCKR-F11, 12	CTGCACTCGTCCCTCTTTCT	GCKR-R11, 12	CGAATGGTTGGGATCAGGAG	11, 12	677
GCKR-F12, 13	CATGGTTTGTTGACTCCTGTGT	GCKR-R12, 13	CTTTTCTTCCACCCTCAGCAC	12, 13	680
GCKR-F13, 14	CACAAGGGCTACTCCTCACTCT	GCKR-R13, 14	ACCACTCCCATCTTCCCTCT	13, 14	699
GCKR-F14	CTTAGCATGGGCAGTGTGGA	GCKR-R14	CTGGATGTGGTTGGTCTTCTCT	14	580
GCKR-F15, 16	CTGGATGGTGAGAGGGAAGAT	GCKR-R15, 16	CCCTACAGCCTTGGGTTTTT	15, 16	566
GCKR-F17	CCTGGTTTACATCTATTGCCCTA	GCKR-R17	AAAAAGAATGAGAGCAACACAG	17	700
GCKR-F18	CCAGTTTAACCCAGCCAGTC	GCKR-R18	AAAAACAGAACCCTGGAGGA	18	672
GCKR-F19	GGGGTTCTTTCTCTGATGACCT	GCKR-R19	GTGTCTGTGTGGGATTGGAGT	19	699

Generation of CFP-GCK and YFP-GKRP vectors

The GFP ORF from pcDNA-DEST53 was removed by restriction digest with SacI (all enzymes New England Biolabs), blunting with Klenow polymerase, and phenol-chloroform: ethanol precipitation followed by DNA purification, subsequent digest with NdeI, and gel-purification of the 6.5kb fragment using a QIAquick gel extraction kit according to the manufacturer's instructions (QIAGEN). pZsYellow1-c1 and pAmCyan1-c1 were cut with BglII, blunted with Klenow polymerase, phenol-chloroform: ethanol precipitated, purified, cut with NdeI, and the 1.1kb fragment was gel-purified. The ZsYellow1 fragment or the AmCyan1 fragment were ligated to the 6.5kb fragment overnight at 12°C with T4 DNA ligase according to the manufacturer's instructions and then transformed into DB3.1

competent cells (Invitrogen) to generate Gateway expression vectors encoding N-terminal YFP or CFP.

Generation of CFP-GCK + pZsYellow1-c1 Gateway co-expression vector

The CFP-GCK promoter, ORF, and polyA signal were removed by digestion with NaeI and NruI. The resulting fragment was cloned into the ZsYellow1-c1 Gateway destination vector using a unique BglII site that was blunted with Klenow polymerase. Insertion orientation was verified by sequencing.

Gateway primer sequences

Human *GCKR* attB1	GGGGACAAGTTTGTACAAAAAAGCAGGCTTAATGCCAGGCACAAAACGGTTT
Human *GCKR* attB2	GGGGACCACTTTGTACAAGAAAGCTGGGTTCACTGAACGTCAGGCTCTAG
Xenopus GCKR attB1	GGGGACAAGTTTGTACAAAAAAGCAGGCTTGATGAGAGGCACAAGGAAGTATC
Xenopus GCKR attB2	GGGGACCACTTTGTACAAGAAAGCTGGGTTCATCGACTCTCCGAGTCC
Human β-cell *GCK* attB1	GGGGACAAGTTTGTACAAAAAAGCAGGCTTAATGCTGGACGACAGAGCCAGG
Human liver *GCK* attB1	GGGGACAAGTTTGTACAAAAAAGCAGGCTTAATGGCGATGGATGTCACAAGG
GCK attB2	GGGGACCACTTTGTACAAGAAAGCTGGGTTCACTGGCCCAGCATACAGG

Site-directed mutagenesis primer sequences

p.Arg51Gln[A]	CTGAGAACATTGTTCAACTGCTAGGGCAATG
p.Glu77Gly	GAGACTCTACAGCGGATCCATTCTGACC
p.Val103Met	CAGATGGGGGGCTGGTTATGCTGAGTGCAG
p.Ser183CysfsX34	CTGTGGGACTCTGCTCCCTTTGTGG
p.Ile219Val	CCAGAAATGACCCCGTTGAAGACTGGAG
p.Gln234Pro	AGTAGCAGAGCGGATGCCGAAAATGCAGGAGAAAC
p.Tyr307Asp	CATCAGGTGACCGACAGCCAAAGCC
p.Thr379AsnfsX36	AGAAGGCTGAGCTCAACCAACCAGGGTCC
p.Pro383Thr	AGCTCACCAACCAGGGTACCCAGTTCACC
p.Ile396Asn	GAGGACTTCCTGACTTCCAACCTTCCCTCTCT
p.Pro446Leu	GTGGGTCAGACCTTGCTGATCCCTCTGAAGAAG
p.Arg478His	CCAGAAGTTCCAGCATGAGCTAAGCACC
p.Ile500Ser	GTGCTTCTTGGTAAGAGCCTACAAAACCACATG

p.Arg540X	CATCGAGAGCCTCCTCTGAGCGATCCACTTTC
p.Arg540Gln	GAGAGCCTCCTCCAAGCGATCCACTTTC
p.His590Tyr	GAGGCTCAGGCATACCTGGCTGCAG
p.Gly607Glu	GAGTGCTCTTGCTGAGCCAGGTCAGAAGC
p.Gly607Val	GTGCTCTTGCTGTGCCAGGTCAGAAG
p.Pro608Ala	GCTCTTGCTGGGGCAGGTCAGAAGC
p.Gly609Ala	CTTGCTGGGCCAGCTCAGAAGCGCACTG
p.Gln610Ala	TGCTGGGCCAGGTGCGAAGCGCACTGCG
p.Gln610Arg	CTTGCTGGGCCAGGTCGGAAGCGCACTGCGGAC
p.Lys611Ala	TGGGCCAGGTCAGGCGCGCACTGCGGAC
p.Arg612Cys	GCCAGGTCAGAAGTGCACTGCGGACCC

[A] Forward PCR primer shown only; reverse primers were the reverse complement of forward primers.

Covariate adjustment for least-square means calculations

	P446L vs WT	L446 vs WT	Rare vs non-rare
Total cholesterol	sex, age at enrollment, statin use, niacin use	sex, age at enrollment, statin use, niacin use	sex, Leu446 alleles, age at enrollment, statin use, niacin use
LDL cholesterol	sex, BMI, statin use, niacin use	sex, BMI, statin use, niacin use	sex, Leu446 alleles, BMI, statin use, niacin use
HDL cholesterol	sex, age at enrollment, BMI, statin use	sex, age at enrollment, BMI, statin use	sex, Leu446 alleles, age at enrollment, BMI, statin use
Triglycerides	sex, race, BMI, statin use, niacin use	sex, race, BMI, statin use, niacin use	sex, race, Leu446 alleles, BMI, statin use, niacin use
CRP		sex, BMI, statin use	

Cohort characteristics for Mexican-American population

	Cases	Impaired FG/GT	Controls
No.	790	338	428
Sex (% Female)	60.1	75.4	68.5
Age in years[A]	46.7 ± 10.9	41.5 ±10.5	37.5 ± 8.9
BMI (kg/m^2)	31.8 ± 6.4	31.0 ± 5.9	29.5 ± 6.5
A1c (%)	10.9 ± 3.7	N/A	N/A

[A] Age at diagnosis for cases; age at examination for controls

Data presented are mean ± SD

Cohort characteristics for Ashkenazi population

	Cases	Controls
No.	951	278
Sex (% Female)	52.2	38.2
Age in years[A]	46.7 ± 10.8	57.3 ± 22.3
BMI (kg/m^2)	30.0 ± 5.6	25.4 ± 4.2
A1c (%)	7.9 ± 1.5	N/A

[A] Age at diagnosis for cases; age at examination for controls

Data presented are mean ± SD

Supplemental References

1. Veiga-da-Cunha, M., and Van Schaftingen, E. 2002. Identification of fructose 6-phosphate- and fructose 1-phosphate-binding residues in the regulatory protein of glucokinase. *J Biol Chem* 277:8466-8473.
2. Rost, B., and Sander, C. 1993. Prediction of protein secondary structure at better than 70% accuracy. *J Mol Biol* 232:584-599.
3. Kim, Y., Quartey, P., Ng, R., Zarembinski, T.I., and Joachimiak, A. 2009. Crystal structure of YfeU protein from Haemophilus influenzae: a predicted etherase involved in peptidoglycan recycling. *J Struct Funct Genomics* 10:151-156.
4. Ramensky, V., Bork, P., and Sunyaev, S. 2002. Human non-synonymous SNPs: server and survey. *Nucleic Acids Res* 30:3894-3900.
5. Ng, P.C., and Henikoff, S. 2001. Predicting deleterious amino acid substitutions. *Genome Res* 11:863-874.